HHS Public Access

Author manuscript

Acta Physiol (Oxf). Author manuscript; available in PMC 2022 July 01.

Published in final edited form as:

Acta Physiol (Oxf). 2021 July ; 232(3): e13672. doi:10.1111/apha.13672.

Aquaporin 4 differentially modulates osmotic effects on vasopressin neurons in rat supraoptic nucleus

Xiaoran Wang[#1], **Tong Li**[#1], **Yang Liu**[#1], **Shuwei Jia**[1], **Xiaoyu Liu**[1], **Yunhao Jiang**[1], **Ping Wang**[2], **Vladimir Parpura**[3], **Yu-Feng Wang**[1]

[1]Department of Physiology, Harbin Medical University, Harbin, China

[2]Department of Genetics, Harbin Medical University, Harbin, China

[3]Department of Neurobiology, The University of Alabama at Birmingham, Birmingham, AL, USA

[#] These authors contributed equally to this work.

Abstract

Aim: Glial fibrillary acidic protein (GFAP) molecularly associates with aquaporin 4 (AQP4) in astrocytic plasticity. Here, we further examined how AQP4 modulates osmotic effects on vasopressin (VP) neurons in rat supraoptic nucleus (SON) through interactions with GFAP in astrocytes.

Methods: Brain slices from adult male rats were kept under osmotic stimulation. Western blot, co-immunoprecipitation, immunohistochemistry and patch-clamp recordings were used for analysis of expressions and interactions between GFAP and AQP4, astrocyte-specific proteins in the SON, as well as their influence on VP neuronal activity. Data were analysed using SPSS software.

Results: Hyposmotic challenge (HOC) of acute SON slices caused an early (within 5 minutes) and transient increase in the colocalization of AQP4 with GFAP filaments. This effect was prominent at astrocytic processes surrounding VP neuron somata and was accompanied by inhibition of VP neuronal activity. Similar HOC effect was seen in the SON isolated from rats subjected to in vivo HOC, wherein a transiently increased molecular association between GFAP and AQP4 was detected using co-immunoprecipitation. The late stage rebound excitation (10 minutes) of VP neurons in brain slices subjected to HOC and the associated astrocytic GFAP's 'return to normal' were both hampered by 2-(nicotinamide)-1,3,4-thiadiazole, a specific AQP4 channel blocker that itself did not influence VP neuronal activity. Moreover, this agent prevented hyperosmotic stress-evoked excitation of VP neurons and associated reduction in GFAP filaments.

Conclusion: These findings indicate that osmotically driven increase in VP neuronal activity requires the activation of AQP4, which determines a retraction of GFAP filaments.

Correspondence Yu-Feng Wang, Department of Physiology, School of Basic Medical Sciences, Harbin Medical University, 157 Baojian Road, Nangang, Harbin150086, China. yufengwang@ems.hrbmu.edu.cn, Vladimir Parpura, Department of Neurobiology, The University of Alabama at Birmingham, 1825 University Blvd, Shelby 1013, Birmingham, AL 35294-0021, USA. vlad@uab.edu.

CONFLICT OF INTEREST

The authors declared that they have no conflicts of interest related to this work.

Keywords

astrocytes; glial fibrillary acidic protein; hyponatraemia; hypothalamus; neuroendocrine system

1 | INTRODUCTION

Adaptive change or plasticity in astrocytic morphology and functions plays pivotal roles in neurochemical regulation of neuronal activity. In astrocytic plasticity, different components of astrocytic proteins exert different roles. Recently, glial fibrillary acidic protein (GFAP), a well-known astrocytic cytoskeletal element, has emerged as an important functional protein. GFAP not only scaffolds the astrocyte shape and anchors tight junctional proteins but also serves as platform to pull different proteins together to facilitate intermolecular interactions [see review in Ref.1]. Moreover, GFAP likely guides the trafficking of membrane proteins including transporters, channels and many others [see review in Ref.2]. Among many GFAP-associated proteins, aquaporin 4 (AQP4), an astrocyte-specific water channel protein,[3] manifests high coordination with GFAP in its spatial localization and volaemic regulation[4] as shown in the supraoptic nucleus (SON) at different stages of suckling stimulation[5] and in rat dams separated from their newborns.[6] In addition, AQP4 can also facilitate clearance of extracellular K^+ and glutamate and may in turn modulate neuronal activity.[7] Therefore, it is possible for AQP4-associated volaemic change to modulate GFAP-associated astrocytic plasticity that, in turn, modulates VP neuronal activity via changing synaptic innervation and intercellular interaction as previously reviewed.[8,9]

In studies of astrocytic-neuronal interactions, osmotic challenge of rat SON has been used extensively. The SON contains two types of magnocellular neurons, vasopressin (VP) and oxytocin neurons. Oxytocin, produced and released from oxytocin neurons, has the main function of controlling maternal behaviour like protection of the newborns and lactation, while VP neurons produce VP, the major humoral factor controlling water absorption in the kidneys and increasing AQP4 expression in the brain.[10] VP neuronal activity is largely determined by the plasticity of their adjacent astrocytes [see review in Ref.9,11]. It is reported that in vitro hyposmotic challenge (HOC) inhibition of VP secretion is a transient event only[12] because of the transient inhibition of VP neuronal activity. In this process, GFAP filaments along astrocytic processes extend to and then retract from the surrounding of VP neurons in the SON.[13] The plastic change in GFAP filaments in the SON also reflects the volaemic changes and morphology of astrocytes as shown in dehydration,[14] during lactation[15] and at different stages of suckling stimulation.[5] However, it remains to clarify whether and how AQP4 activity influences GFAP expression in astrocytic modulation of VP neuronal activity in acute physiological processes.

To assess this issue, we examined the interaction between GFAP and AQP4 in the SON of rats that received HOC. The finding indicates that AQP4-associated volaemic change in astrocytic processes is critically involved in astrocytic sensation and/or transduction of osmotic signals and regulation of VP neuronal activity, partially by modulating GFAP plasticity.

2 | RESULTS

2.1 | HOC causes redistribution of AQP4 that corresponds to GFAP spatiotemporal dynamics in the SON

HOC in vitro and in vivo transiently increases GFAP levels in the SON, which then returns to the control/base levels.[13] Variation on GFAP levels underlies astrocytic morphological plasticity.[16,17] During suckling, there is a spatiotemporal GFAP redistribution in the SON, which is accompanied by synergistic changes in AQP4 distribution.[5] Thus, we hypothesized that AQP4 distribution is also associated with GFAP dynamics during HOC. Consequently, we examined spatiotemporal distribution of AQP4 and GFAP filaments in the SON after in vitro and in vivo HOC using immunostaining. Under control conditions, AQP4 was mainly located at astrocytic somata (Figure 1). Five minutes of in vitro HOC significantly increased GFAP-associated AQP4 stain level (n = 6, $P < .05$), particularly around VP neuronal somata. At 20 minutes of in vitro HOC, GFAP-associated AQP4 stain subsided to control levels (Figure 1A). Ten minutes of in vivo HOC also significantly increased GFAP-associated AQP4 stain in the SON when compared to that at 10 minutes of iso-osmotic treatment. At the late stage of in vivo HOC (30 minutes), GFAP-associated AQP4 stain intensity returned to the level seen in 30 minutes iso-osmotic control (Figure 1B). Throughout the HOC, there was an additional marked redistribution of AQP4. At 10 minutes of HOC, AQP4 intensity at (GFAP-positive) astrocytic processes that surrounded neurophysins-positive somata of magnocellular neurons was increased as compared to that at 10 minutes control (Figure 1Ba, n = 6, $P < .01$). Interestingly, at 30 minutes of HOC (Figure 1Ba), there was a re-distribution of AQP4 stain, which markedly accumulated at astrocytic end feet, plastering blood vessels, as compared to its location in the SON at the early time points (Figure 1Ba). Statistically, this end feet-associated AQP4 intensity was 238.5 ± 14.4% of that at 10 minutes (n = 6, $P < .05$), but it was insufficient to cause the change in the entire GFAP-associated AQP4 signal (~130%, Figure 1Bb). Of note, in our experimental paradigms, 10 minutes (early) and 30 minutes (late) time points of in vivo HOC correspond to 5 and 20 minutes time points of HOC in vitro, respectively. This time lag is as a result of the fact that in vitro HOC can immediately exert effect while the in vivo HOC takes ~10 min to lower plasma osmotic levels by 10–20 mOsm/kg, as we reported elsewhere.[13] Nonetheless, this time course of GFAP-associated AQP4 dynamics in the SON under HOC challenge in vivo and in vitro matches that of changes in GFAP levels itself (Figure 1Bb). The changes in GFAP levels here were consistent with our pervious study.[13] The sole exception in the present work was that GFAP filaments at late HOC in vitro displayed significant ‘undershoot’, while such decrease in the GFAP filaments was previously only seen as a trend (compare Figure 1Ab here and Figure 2Ba in Ref.13). This difference should not distract from the finding that AQP4 associated with GFAP matches GFAP temporal dynamics during prolonged HOC both in vivo and in vitro.

To examine if the spatiotemporal course of GFAP and AQP4 dynamics might represent their functional association between GFAP and AQP4 expressions, we quantitated AQP4 in Western blots. There was no significant change in total AQP4 levels in the SON over the HOC at 10 minutes (98.3 ± 7.8% of iso-osmotic control, n = 6, $P > .05$, Figure 2A). Next, we examined molecular associations between GFAP and AQP4 using co-

immunoprecipitation approach. The result showed that the two molecules had not only molecular association but also showed synergistic changes with their levels over the HOC: there were initial increase and then return to the basal level (Figure 2B). Additionally, co-immunoprecipitation results from HOC in vivo, at 10 minutes interval, showed an increased molecular association between GFAP and AQP4 when compared to data obtained from animals receiving iso-osmotic treatment (Figure 2C; n = 3, $P < .05$). This increased association between GFAP and AQP4 is consistent with the increased colocalization of the two molecules in astrocytic processes.

2.2 | Effects of blocking AQP4 activity on VP neuronal responses to HOC

The timing of HOC-induced transient increase in GFAP level corresponds to the decreased firing activity of VP neurons and it requires intact astrocytic functions.[13] The strong association of AQP4 with GFAP and the determining effect of AQP4 in astrocytic volaemic change[1,18] further suggest AQP4 involvement in astrocytic modulation of VP neuronal activity. To test this possibility, we recorded, in a whole-cell patch-clamp configuration, activity of VP neurons in the SON slices subjected to the HOC and examined the effect of an AQP4 blocker, 2-(nicotinamide)-1,3,4-thiadiazole (TGN-020), on HOC-modulated VP neuronal activity. We selected to investigate a subset of SON magnocellular neurons in acute brain slices (in vitro) that showed phasic firing at rest/baseline, an unequivocal characteristic of VP neurons (Figure 3A, baseline) [reviewed in Ref.19-22]. Having established stable whole-cell patch-clamp recordings of VP neurons, we exposed the SON brain slices to hyposmotic artificial cerebrospinal fluid (aCSF), which represented the HOC (Figure 3A,B). Consistent with our previous work,[13] HOC caused a dual response in VP neurons. There was an initial reduction or valley in the firing rate (Figure 3A-C) followed by a rebound of the firing rate, seen as an increased ‘peak’ rate of action potential (AP) discharges when compared to the baseline (Figure 3A-C). After washout, the firing rate of VP neurons returned to control levels (Figure 3A, washout).

Inhibition of the firing rate of VP neurons (n = 9) occurred within 0.5–5 minutes (Median: 1.5 minutes, interquartile range or IQR: 0.6–2.9 minutes) of the HOC, and the rebound increase in the firing rate occurred within 8–10 minutes (Median: 8.75 minutes, IQR: 8.0–9.9 minutes) of the HOC onset. Statistically, there was significant difference ($P < .001$ by one-way repeated measures analysis of variance or rANOVA) in the firing rate between the baseline (4.97 ± 1.08 Hz, n = 9) and the valley (2.92 ± 1.11 Hz, $P = .011$ by Bonferroni test) or the peak (6.52 ± 1.00 Hz, $P = .025$ by Bonferroni test) after HOC. Moreover, the firing rate returned to the baseline level after 10 minutes washout with iso-osmotic aCSF (5.59 ± 0.95 Hz, $P = .958$ by Bonferroni test). Consistent with the changes in the firing rate, HOC also significantly ($P < .001$ by rANOVA) decreased the decay slope of afterhyperpolarization (AHP) at the valley of firing activity (the valley 0.066 ± 0.008 mV/ms vs the baseline 0.096 ± 0.015 mV/ms, $P = .047$ by Bonferroni test) and increase the decay slope of AHP at the rebound of firing activity (0.131 ± 0.015 mV/ms, $P = .032$ by Bonferroni test), which became insignificant after washout (0.093 ± 0.019 mV/ms, $P = 1.000$ by Bonferroni test). HOC also significantly ($P = .001$ by rANOVA) increased the full width at half maximum (FWHM) of AHP at the valley of firing activity (62.0 ± 7.6 ms vs the baseline 45.3 ± 5.2 ms, $P = .010$ by Bonferroni test) and decreased the FWHM of AHP

at the rebound of firing activity (34.0 ± 3.9 ms, $P = .005$ by Bonferroni test), which became insignificant after washout (42.8 ± 3.6 ms, $P = .916$ by Bonferroni test). However, there were no significant changes in the amplitude and duration of APs and the amplitude of AHPs (Figure 3D).

Under iso-osmotic condition, TGN-020 (10 μmol/L, 10 minutes) had no significant effect on the firing rate ($P = .606$ by paired *t* test), the AP amplitude ($P = .849$ by paired *t* test) and FWHM/duration ($P = .302$ by paired *t* test), and the AHP amplitude ($P = .176$ by paired *t* test), FWHM ($P = .718$ by paired *t* test) and decay slope ($P = .891$ by paired *t* test, Figure 4).

In the presence of TGN-020 (10 μmol/L, 10 minutes before, during and after HOC), inhibitory responses of VP neurons to HOC, ie the reduction in firing rate became insignificant at 1.5 minutes of HOC (7.20 ± 1.10 Hz in baseline vs 6.55 ± 1.13 Hz in HOC, n = 10, $P = .180$ by Bonferroni test). HOC-evoked reduction in the firing rate did not occur in the presence of TGN-020 until 10 minutes when significant difference ($P = .019$ by rANOVA) in the firing rate appeared between the baseline and 10 minutes after HOC (4.85 ± 0.96 Hz, $P = .009$ by Bonferroni test). However, the rebound increase in the firing rate was absent in 9 of the 10 cells ($P < .05$ by chi-square test). The firing rate returned partially to baseline level after 10 minutes washout with iso-osmotic aCSF plus TGN-020 (5.55 ± 0.96 Hz, $P = .180$ to the baseline by Bonferroni test; Figure 5A-D). There was significant decrease ($P = .002$ by rANOVA) in the AP amplitude between the baseline (54.2 ± 4.9 mV, n = 10) and 10 minutes after HOC (40.0 ± 4.9 mV, $P = .029$ by Bonferroni test). The change in AP amplitude was insignificant at 1.5 minutes of HOC (49.7 ± 4.6 mV, $P = .151$ by Bonferroni test) and returned partially to baseline level after 10 minutes washout (42.9 ± 4.4 mV, $P = .037$ by Bonferroni test). There was significant increase ($P = .011$ by rANOVA) in AP FWHM between the baseline (2.60 ± 0.21 ms, n = 10) and 10 minutes after HOC (3.28 ± 0.29 ms, $P = .040$ by Bonferroni test). The change in AP FWHM was insignificant at 1.5 minutes of HOC (2.81 ± 0.29 ms, $P = .167$ by Bonferroni test) and returned partially to baseline level after 10 minutes washout (2.99 ± 0.28 ms, $P = .070$ by Bonferroni test). In the presence of TGN-020, 10 minutes of HOC significantly ($P = .001$ by rANOVA) decreased the decay slope of AHP (0.065 ± 0.015 mV/ms vs the baseline 0.128 ± 0.018 mV/ms, $P = .005$ by Bonferroni test), but was insignificant after 1.5 minutes of HOC (0.108 ± 0.021 mV/ms, $P = .581$ by Bonferroni test) and washout (0.108 ± 0.020 mV/ms, $P = .427$ by Bonferroni test). There was significant difference ($P = .005$ by rANOVA) in the AHP FWHM between the baseline (40.9 ± 3.7 ms) and 1.5 minutes after HOC (45.4 ± 4.4 ms, $P = .026$ by Bonferroni test) or 10 minutes after HOC (71.2 ± 10.2 ms, $P = .017$ by Bonferroni test). The AHP FWHM returned to baseline level after 10 minutes washout (42.0 ± 4.0 ms, $P = 1.000$ by Bonferroni test). However, there were no significant changes in the amplitude of AHP ($P = .136$ by rANOVA). These findings are consistent with the pivotal roles of AQP4 in the regulatory volume decrease (RVD).[18]

2.3 | Effects of blocking AQP4 activity on VP neuronal responses to hyperosmotic stress

To test whether AQP4-associated astrocytic plasticity is a common regulatory factor of VP neurons, we further tested effects of TGN-020 on hyperosmotic stress-evoked excitation of VP neurons.[23,24] As shown in Figure 6A and B, hyperosmotic stress significantly ($P = .007$

by rANOVA) increased the firing rate of VP neurons (4.66 ± 1.47 Hz in the baseline vs 6.68 ± 1.37 Hz at 10 minutes after hyperosmotic stress, n = 6, $P = .008$ by Bonferroni test; 4.98 ± 1.09 Hz at 10 minutes washout, $P = 1.000$ compared to the baseline by Bonferroni test). Further analysis revealed that hyperosmotic stress also significantly reduced AHP duration ($P = .022$ by rANOVA) and AHP decay slope ($P = .005$ by rANOVA; Figure 6C).

Similar to the effect on HOC action, TGN-020 also blocked hyperosmotic excitation of VP neurons (Figure 7A, B). In the presence of TGN-020 (10 μmol/L, 10 minutes before hyperosmotic excitation), excitatory responses of VP neurons became insignificant in the 6 neurons tested. Statistically, there was no significant difference ($P = .304$ by rANOVA) in the firing rate between the baseline (6.51 ± 1.80 Hz, n = 6), and 10 minutes after hyperosmotic stress (7.67 ± 2.32 Hz) or after washout (7.30 ± 1.94 Hz) (Figure 7C). There was also no significant difference in other parameters ($P = .356$ for AP amplitude, $P = .142$ for AP duration, $P = .406$ for AHP amplitude, $P = .200$ for AHP duration, $P = .450$ for AHP decay slope, by rANOVA; Figure 7C). The blocking effect of TGN-020 on osmotic excitation of VP neurons is consistent with the view that AQP4 is a critical component of osmosensation and astrocytic plasticity[25] that determines the osmotic regulation of VP neuronal activity.[1]

2.4 | Effects of blocking AQP4 activity on HOC-elicited GFAP retraction

AQP4-associated ion channel activity[18] could also modulate GFAP expression through changing astrocytic volume and intracellular ionic environment.[2,25] To test the latter possibility, we quantified GFAP expression levels and patterns in the SON using immunohistochemistry and confocal microscopy in vitro using brain slices from 13 rats. The presence of TGN-020 did not significantly influence HOC-elicited GFAP expansion at 5 minutes; however, HOC-evoked GFAP retraction at 20 minutes did not occur (Figure 8A). By contrast, hyperosmotic stress for 20 minutes caused significant retraction of GFAP filaments (Figure 8B) as previously reported.[23] However, in the presence of TGN-020, hyperosmotic stress failed to cause such reduction. These finding are in agreement with that AQP4 is a critical molecule determining the RVD and astrocytic volaemic changes.[1,18]

3 | DISCUSSION

Present findings confirm a dual effect of HOC on GFAP and AQP4 expressions, and molecular and functional associations between the two molecules in osmotic modulation of VP neuronal activity. This study highlights a pivotal role of AQP4 activity in GFAP-associated retraction of astrocytic processes and the subsequent increase in VP neuronal activity (Figure 9).

Decreases in blood osmolality allow excessive water to enter the brain, thereby creating a hyposmotic environment around neurons and causing brain oedema.[25] The present work simulates the pathogenesis of hyponatraemia-evoked brain oedema with HOC and confirms a dual cellular volume regulation: swelling and the ensuing RVD in both astrocytes and neurons.[26] Relative to the low permeability of VP neurons to organic osmolytes[27] and volume constancy of neurons in HOC,[28] astrocytes are more sensitive to the osmotic change as a result of their ability to rapidly take up excessive water and ions through AQP4 and

associated ionic channels.[1] The rapid changes in GFAP are reasonable since GFAP plasticity has been previously identified in the SON as results of polymerization/depolymerization and/or changes in catabolism of GFAP.[5,29] Moreover, the coordinated redistribution of GFAP and AQP4 in astrocyte processes supports the view that GFAP plasticity determines astroglial shape and functions via its scaffolding and guiding roles as previously proposed.[2,4]

The effect of HOC on GFAP/astrocyte morphology is rate-dependent, similar to the profile of VP release in hypothalamic explants as previously identified[12] and analysed.[1] This notion is supported by the findings that HOC-evoked cell swelling and the ensuing RVD take only seconds to minutes in cell cultures;[30] that in slices, 5 minutes is necessary to evoke significant GFAP increase; and that in whole animals, GFAP increase needs 10 minutes to be significant. The HOC effect is also related to the nature of assays. In the hypothalamic explants,[12] the inhibition of VP release reaches the valley between 20 and 60 minutes, whereas the decrease in spiking bottoms at 5 minutes and recovers by 10 minutes in slices.[13,31] This apparent discrepancy is related to the time needed for HOC to infiltrate thick tissue before reaching all VP neurons. With these facts in mind, it would not be a surprise to see the prolonged time course (≥24 hours) for the occurrence of brain oedema and the ensuing reversal of VP secretion in patients with water-retaining diseases,[32] in which a reduction in osmolality by 5–10 mOsm/kg leads to serious hyponatraemia.

Differences in osmotic responses in GFAP expression between in vivo and in vitro could partially account for the persistent inhibition of VP neurons in the hyposmotic rat model.[31] Both in vivo and in vitro HOC transiently increased GFAP filaments; however, complete reversal of GFAP filament increases did not occur in vivo. According to the general relationship between astrocyte morphology and neuronal functions,[8] a slower, incomplete, reversal of GFAP-guided expansion of astrocyte processes should favour VP neuronal activity, so should favour VP release. Under different in vivo conditions, this delayed GFAP plasticity might be modulated differently from that in vitro. In the in vivo hyposmotic rat model[33] elicited with desmopressin, a V2-type VP receptor agonist, the resultant water retention could in turn facilitate a prolonged elongation of GFAP filaments and could persistently inhibit VP neuronal activity. In addition, increased water transfer between neural tissue and circulation should also alleviate the HOC in the brain in whole animals. As shown in Figure 1A, increased AQP4 around blood vessels after longer in vivo HOC may indicate increase in water transfer through astrocytes to the circulation. With normal functional heart and kidneys, the excess water tends to be removed, thereby reducing the speed of osmolality reduction, GFAP/astrocytic plasticity and rebound of VP release. However, in water-retaining diseases, these processes are not available because of serious organ failure and presence of numerous neurohumoral factors that facilitate VP release[11] and, thus, result in VP hypersecretion.

It is known that GFAP plasticity largely determines the extension and retraction of astrocytic processes.[34] This GFAP function is in association with changes in AQP4 expression and actin filaments in the SON.[5] In our observation, HOC also causes a transient increase in AQP4 expression in parallel with GFAP expression (Figure 1 and 2). Increase in GFAP expression could account for an increased membrane insertion of AQP4 and cell swelling since astrocyte swelling evoked by high K^+ and hyposmotic solution is significantly slower

in GFAP-deficient mice.[35] Similarly, a reduction in GFAP facilitates the RVD since during retraction of astrocyte processes, the molecular association between GFAP and actin increased significantly.[5] It is possible that while GFAP retracts from astrocyte processes, the membrane of astrocytic processes would collapse via the contraction of GFAP-associated actin and AQP4. Moreover, the decreased association of GFAP with AQP4 and relocation of AQP4 to astrocytic end feet apposing blood vessels will help transfer of water from neurons to blood vessels. Thus, GFAP-guided glial retraction is functionally synergistic with the RVD.

AQP4 is a critical molecule determining the RVD and astrocytic volaemic changes. The present study further validates the functional involvement of AQP4 activity in osmotic regulation of VP neuronal activity by showing that TGN-020 blocked both the rebound excitation following HOC and the hyperosmotic excitation of VP neurons. Moreover, the blocking effect of TGN-020 on GFAP retraction around VP neurons during HOC (20 minutes) and hyperosmotic stress indicates the mediating role of AQP4 on GFAP retraction. As previously reviewed,[4] AQP4 is functionally coupled with many ion channels and transporters and its opening for water flux is accompanied with changes in ion concentration in astrocytes that could change GFAP metabolism and assembly. Benfenati and colleagues reported that AQP4 can cause RVD and increase intracellular Ca^{2+} by coupling with transient receptor potential vanilloid [43,36], albeit this coupling is not necessary.[18] Increased intracellular Ca^{2+} level is a critical step for GFAP depolymerization via protein kinase A and other signalling process,[25,37] and thus, AQP4 blockage could elongate the GFAP filament extension.

The dual change in GFAP and AQP4 during HOC is in agreement with the dual alteration of VP neuronal activity. Initially, increased association between GFAP and AQP4, particularly at areas close to neuronal somata, can bring more AQP4 to astrocytic processes and pass more water into the expanding processes. Increases in AQP4 also facilitate clearance of extracellular K^+ and glutamate,[7] and thus enforce the suppressive effects of HOC on VP neuronal activity. The late reduction in AQP4 expression around neuronal somata may reduce the removal of extracellular K^+ and glutamate, which facilitates the rebound of VP secretion. Notably, blocking AQP4 does not significantly influence the firing activity of VP neurons directly; however, it reduces spike amplitude and increased spike duration/FWHM in the presence of This finding indicates that under iso-osmotic condition, AQP4 does not influence astrocytic morphological plasticity and VP neuronal activity; however, under HOC, water flux through AQP4 contributes to astrocytic plasticity and VP neuronal activity. As HOC also creates lower Na^+ levels around VP neurons and hence reduces Na^+ gradient across the plasma membrane, which reduces AP amplitude. The low extracellular Na^+ also decreases the screening effect of Na^+ on Ca^{2+} influx,[38] which causes relative increases in Ca^{2+} influx through NMDA receptor channel and, together with reduction in K^+ efflux, results in spike broadening. Since HOC-evoked retraction of astrocytic processes is also blocked in the presence of TGN-020, RVD and its excitatory effect on VP neurons do not occur. In addition, GFAP and the ensuing astrocytic morphological plasticity can also modulate VP neuron activity via changing synaptic innervations, glutamate metabolism and junctional communications of SON neurons.[39] Withdrawal of glial processes from the interneuronal space increases direct appositions among neurosecretory cells. The increase in

direct soma-somatic apposition (7–9 nm separation) of neurosecretory cells could produce a tonic rise in extracellular K^+ levels which would increase protein synthesis and contribute to the raised excitability of these neurons. Also, the removal of interposed glia promotes the formation of gap junctions and shared synapses among these neurons. These in turn participate in producing the coordinated firing that maximizes hormone release. Thus, changing these processes is likely involved in the effect of blocking AQP4 on VP neuronal activity as well.

From the electrophysiological recording data, differences in VP neuronal activity mainly reside in the recovery rate of AHP. This AP's undershoot phase can be classified into 'fast', medium' and 'slow' components. While fast and medium AHPs can be generated by single APs, slow AHPs generally develop only during trains of multiple APs. In our observations, the AHP mainly fell in the classification of medium AHP. Notably, the presence of TGN-020 mainly influences HOC-modulated AHP duration but not the amplitude. This finding is in agreement with a report on the responsive feature of 'phasic neurons' to inflammatory stimulation where complete Freund's adjuvant or bee venom toxin melittin treatments significantly enhance amplitudes of AHP in tonic firing neurons but not in phasic neurons.[40] The initial elongation and late shortening of AHP duration are consistent with the initial reduction and then increase in AP frequency since AHP duration is a major determining factor for the firing rate.[41] The reason for TGN-020 reversal of the reduction in AHP duration could result from the loss of AQP4 modulation of astrocytic osmotic balance and morphological plasticity. The effects of hyperosmotic stress on AHP duration and decay slope as well as the blockade effect of TGN-020 are consistent with the findings in HOC. It is known that K^+ channels activated by depolarization mediate the fast AHP that regulates the interval between adjacent spikes. The medium AHP is mediated by Ca^{2+}-activated K^+ channels of vertebrate neurons; these channels are sensitive to apamin and N-type Ca^{2+} channel blockers.[42] After blocking AQP4, increased intracellular Ca^{2+} level in HOC[38] further activates Ca^{2+}-activated K^+ channels, thereby elongating the duration of this medium AHP. Resultantly, the late rebound increase in AP frequency of VP neurons fails to occur.

Our previous study[13] presented that putative oxytocin neurons exhibit a different pattern of response from that of VP neurons to the HOC, ie prolonged inhibition without rebound increase in the firing rate. Obviously, the retraction of astrocytic processes during RVD should exert a facilitatory influence on activity and secretion of oxytocin neurons in view of the spatial relationship between oxytocin neurons and astrocytes.[9] However, the lack of rebound of oxytocin secretion suggests that some inherent features of oxytocin neurons may play a dominant role in the response to HOC. It is known that VP neurons and oxytocin neurons express different types of ion transporters, ie Na^+-K^+−$2Cl^−$ cotransporter 1 in VP neurons responsible for $Cl^−$ import and the K^+-$Cl^−$ cotransporter 2 in oxytocin neurons for $Cl^−$ export.[43] This feature makes oxytocin but not VP neurons to present inhibitory response to the increase in extracellular GABA and taurine that are released during RVD.[37] Another difference in oxytocin neurons from VP neurons to HOC is that swelling-induced oxytocin secretion from the SON and PVN does not occur unless Ca^{2+} influx is reduced in the presence of Ca^{2+}-free medium or inhibition of stretch-activated channels by $GdCl_3$.[44] This suggests that persistently reduced oxytocin secretion during HOC is associated with reduction in Ca^{2+} influx; however, the detailed mechanisms remain to be explored.

Notably, VP secretion is determined not only by the firing rate and pattern of VP neurons but also by the physiological status on nerve endings and pituicytes (astrocyte-like cells) in the neurohypophysis. The neurosecretion of nerve endings is mainly driven by APs propagated down the axons from the somata in the SON and PVN while it is also modulated by the status of pituicytic plasticity. AQP4 is expressed in some GFAP-positive pituicytes.[45] In mouse pituitary, AQP4 is abundant, mainly in the neural lobe, distributed along pituicytes' plasma membranes that are in close contact with nerve terminals and fibres; after chronic osmotic stimulation with salt loading for 8 days, AQP4 immunolabelling is enhanced.[46] Because the morphological plasticity of pituicytes is reminiscent of that of astrocytes in the SON in response to hyperosmotic stress,[47] we tentatively suggest that AQP4 plays a similar role in osmotic regulation of VP secretion in the neurohypophysis as astrocytes around VP neurons do. However, as AQP4 expression in grey matter is different from that in white matter astrocytes in brain oedema,[48] it remains to be examined if AQP4 expression in the neurohypophysis is different from that in the SON.

Taken together, prolonged HOC can change VP neuronal activity by modulating astrocytic morphologic plasticity and the ensuing glial neuronal interactions via GFAP-guided AQP4 expression. These findings provide a novel cellular mechanism (Figure 9) to explain the dual effect of HOC on VP secretion in hypothalamic explants.[12] In addition, these findings also add new facet in explaining the pathogenesis of inappropriate VP secretion in water-retaining diseases with hyponatraemia.[11,25,32]

4 | MATERIALS AND METHODS

4.1 | Animals

Male Sprague-Dawley rats (290–310 g) were used in this study. All animal procedures were in accordance with the National Institutes of Health Guide and approved by the Institutional Animal Care and Use Committees of Harbin Medical University and University of Alabama, Birmingham.

4.2 | HOC and tissue sampling

Methods of in vivo HOC were identical as in our previous report.[13] Briefly, after urethane anaesthesia, rats were intraperitoneally injected with either iso-osmotic solution (0.9% w/v NaCl, control) or H_2O (HOC) each at 20 mL/kg. Water application resulted in a reduction in serum osmolality by 11–15 mOsm/kg within 10–30 minutes. Rats were then decapitated using a guillotine at three time points: 0, 10 or 30 minutes after the injection. Hypothalamic blocks were dissected and then set in an oxygenated (bubbled with 95% O_2/5% CO_2 gas mixture) aCSF for 1–2 minutes before further processing. The regular (control) iso-osmotic (305 mOsm/kg) aCSF contained (in mM): 126 NaCl, 3 KCl, 1.3 $MgSO_4$, 2.4 $CaCl_2$, 1.3 NaH_2PO_4, 26 $NaHCO_3$, 10 Glucose and pH 7.4.

For in vitro osmotic experiments, rat brains were quickly dissected after decapitation and immersed in ice-cold slicing solution that was oxygenated through bubbling with a compressed gas mixture of 95% O_2/5% CO_2. The slicing solution contained one-third of 10% sucrose and two-thirds of regular aCSF. Coronal slices (200 μm thick) were obtained

from the SON as previously described.[5] After pre-incubation in regular aCSF at room temperature (22–24°C) for ~1 hour, slices were treated with hyposmotic, iso-osmotic or hyperosmotic aCSF (275, 305 or 335 mOsm/kg, respectively) for 0, 5 and 20 minutes at 32°C. The hyposmotic aCSF (275 mOsm/kg) was prepared by reducing NaCl to 111 mmol/L from the regular aCSF and the hyperosmotic aCSF (325 mOsm/kg) was prepared by increasing NaCl to 141 mmol/L from the regular aCSF.

4.3 | Immunohistochemistry

To examine the distribution of GFAP and AQP4, we performed immunostaining and confocal microscopy as previously reported.[5] Briefly, for in vivo experiments, hypothalamic blocks were fixed in 4% paraformaldehyde [pH 7.4 in 0.1 mol/L phosphate buffered saline (PBS)] for ~72 hours at 4°C and then sectioned into slices of 50 μm thickness. For in vitro studies, pre-sectioned 200-μm-thick slices were fixed in the 4% paraformaldehyde solution for ~24 hours at 4°C. Following fixation, slices were subjected to cell permeation with 0.3% Triton X-100 and blockade of non-specific antibody binding sites with 0.3% gelatin (w/v in PBS), and then were incubated overnight at 4°C with primary antibodies (both at 1:300 dilution in gelatin-PBS) against GFAP (Santa Cruz Biotechnology Inc, Cat. No. SC-33673) and AQP4 (Alomone, Cat. No. AQP-004). We co-applied primary antibodies against VP neurophysin (VP-NP, Cat. No. SC-27093) and those against the oxytocin carrier, neurophysin I (1:300; Cat. No. SC-7810), to obtain labelling of both neurophysins (NPs) and, thus, all magnocellular neurons.[5] After washing, slices were incubated for 1.5 hours at room temperature with appropriate secondary antibodies conjugated with Alexa Fluor ® 488 (GFAP), 555 (AQP4) or 647 (NPs) (Invitrogen; all at 1:1000 dilution in gelatin-PBS with 0.1% Tween-20). Hoechst (bisbenzimide H 33342 trihydrochloride, Sigma, Cat. No. B2261; 0.5 μg/mL for 15 minutes) was used to label cell nuclei. Small homogeneous, round or elliptical, nuclei were considered as astrocytic nuclei (and were additionally associated with positive GFAP stain), while big (>8 μm), round heterogeneously stained nuclei were considered as magnocellular neuron nuclei, as previously described.[49] For colocalization of AQP4 with GFAP surrounding magnocellular somata, we used only GFAP filaments that were longer than 50 μm and wider than 2 μm. Fluorescence of different labels was sequentially scanned with a multi-channel laser scanning confocal microscope (Leica TCP SP2) at 0.5 or 1 μm z-axis sections. To visualize the effect of AQP4 blocker on GFAP staining, we used both a fluorescence microscope (Eclipse FN1, Nikon) equipped with a charge-coupled device camera (DS Ri2, Nikon) and a confocal microscope (Thorlabs). To assure the comparability of fluorescence measurements between various groups, slices among different treatments were matched in size/location of imaging fields. Additionally, the same scanning/imaging conditions were applied. Control experiments to exclude non-specific staining included pre-adsorption of primary antibodies with antigenic peptides and application of secondary antibody after omitting the primary antibody.

4.4 | Western blots

We obtained SON proteins for Western blot analysis as previously described.[29] Briefly, the SON was punched out of hypothalamic blocks or slices with little of perinuclear zone tissue, which was then lysed and centrifuged to remove insoluble components. Concentration of soluble proteins was assayed using the bicinchoninic acid protein assay reagent (Thermo

Scientific Pierce). In each condition and time point, 60 μg of protein per lane was separated on a 10% sodium dodecyl sulphate-polyacrylamide gel electrophoresis and then transferred onto a polyvinylidene difluoride membrane (Millipore) at 4°C. Membranes containing proteins were first treated with 5% fat-free dry milk (w/v in PBS) for 1 hour at room temperature, and then incubated with primary antibodies (against GFAP and AQP4, 1:500 dilution). Actin was probed using an anti-actin antibody (Cat. No. SC-1616, 1:500) and used as loading control. Protein immunoblotting bands were visualized using horseradish peroxidase-conjugated secondary antibodies and an enhanced chemiluminescence detection system.

4.5 | Co-immunoprecipitation

The SON tissue was isolated as for Western blots stated above. Total lysates were pre-cleared with protein A agarose (Millipore), and then 1.5 μg of immunoprecipitating antibody against GFAP was added to the SON lysate containing 1.0–1.5 mg of protein to form immune complexes. After overnight incubation at 4°C, the immune complexes were captured by adding 50 μL of protein A agarose bead slurry through gently rocking the incubation for 2 hours at 4°C. The protein-loaded agarose beads were then collected and washed before being re-suspended in sample buffer and boiled for 10 minutes. The beads were then removed by centrifugation and the supernatant was run on a 10% sodium dodecyl sulphate-polyacrylamide gel electrophoresis. Following electrophoresis, proteins were transferred onto membranes, which were sequentially probed with antibodies against GFAP or AQP4 (both at dilution of 1:300) for 4 hours at room temperature, each followed by secondary antibodies and enhanced chemiluminescence detection. Positive and negative controls consisted of total lysates and non-specific IgG respectively; actin immunoreactivity was used as loading control. All reagents were from GE Healthcare.

4.6 | Patch-clamp recordings

Patch-clamp recording procedures were similar to those described previously.[13] That is, 300-μm-thick coronal brain slices were pre-incubated at room temperature for 1 hour in oxygenated regular aCSF after dissecting the hypothalamus and before drug treatment or application of other procedures. Slices were then transferred into a recording chamber and superfused with normal aCSF at 35°C at a rate (2.5–3 mL/min) faster than that (1.2–1.5 mL/min) in our previous studies.[13] Whole-cell patch-clamp recordings were obtained from magnocellular neuronal somata of the SON with Multiclamp 700B amplifier (Molecular Devices). The pipette solution contained (in mM): 145 K-gluconate, 10 KCl, 1MgCl2, 10 HEPES, 1 EGTA, 0.01 CaCl2, 2 Mg-ATP, 0.5 Na2-GTP and pH 7.3, adjusted with KOH. For identifying the chemical nature of recorded neurons, 0.05% biocytin (B4261, Sigma, USA) was added to the pipette solution. Signals that were filtered, sampled at 5 kHz and analysed offline using Clampfit 10 software (Molecular Devices). The firing rate, ie AP discharges (f, Hz), was calculated every 0.5 minutes. An increase or a decrease in the firing rate was considered if the number of AP discharge/s (Hz) changed more than 3 SEM of the firing rate at rest, in preceding 2 minutes section. In the heatmaps, the relative firing rate was calculated as $(f - f_0)/f_0$, where f_0 was the baseline firing rate (Hz) averaged over a 5 minutes prior to HOC or hyperosmotic stress. Duration of APs and AHP was expressed as the full width of respective events at FWHM (ms). Decay slope of AHP was defined based on 90%

and 10% values of the AHP peak amplitude. We used recordings obtained from VP neurons only. These neurons were mainly classified based on their phasic firing at rest, which is an unequivocal characteristic of VP neurons in our experimental conditions (reviewed in Ref.21,50). In SON neurons that did not show typical phasic firing, post hoc immunostaining was performed using conventional avidin-biotin complex method.

4.7 | Data collection and analysis

Analyses of data took the same methods as previously described.[5,13] To assay GFAP expression in single optical sections, whole frame of the image was compared on the same background level of fluorescence intensity. Assessing blood vessel-associated AQP4 intensity was based on the presence of AQP4 stain independent of neuronal somata. The efficiency of this single optical section-based analysis in reflecting GFAP plasticity had been validated by three-dimensional reconstructions and fluorescence microscopy.[5] In evaluation of AQP4 stains surrounding VP neurons, only stains that had a length of longer than half VP neuronal somata were counted.

Raw data were normalized to the controls prior to statistical testing. One-way repeated measures analysis of variance followed by Bonferroni test for multiple comparisons were used for statistical analyses (Sigma Stat software program); paired t test was used to analyse paired samples; $P < .05$ was considered significant. All measurements are expressed as mean ± SEM except otherwise stated in the Results, ie IQR that show the median (middle value) of the lower and upper half of the data.

Supplementary Material

Refer to Web version on PubMed Central for supplementary material.

ACKNOWLEDGEMENTS

This work was supported by the higher education talents funds of Heilongjiang province (grant No. 002000154, YFW) and the fund of ‘Double-First-Class’ Construction of Harbin Medical University (key laboratory of preservation of human genetic resources and disease control in China). Vladimir Parpura’s work is supported by a grant from the National Institute of General Medical Sciences of the National Institutes of Health (R01GM123971). We thank Dr Runsheng Jiao, Chunmei Hou and Jiawei Yu for discussion. Vladimir Parpura is an Honorary Professor at University of Rijeka, Croatia.

Funding information

National Institute of General Medical Sciences of the National Institutes of Health, Grant/Award Number: R01GM123971 (VP); “Double-First-Class” Construction of Harbin Medical University (Songbin Fu); Higher Education Talents Funds of Heilongjiang Province, Grant/Award Number: 002000154 (YFW)

REFERENCES

1. Wang YF, Parpura V. Astroglial modulation of hydromineral balance and cerebral edema. Front Mol Neurosci. 2018;11:204. [PubMed: 29946238]
2. Li D, Liu X, Liu T, et al. Neurochemical regulation of the expression and function of glial fibrillary acidic protein in astrocytes. Glia. 2020;68(5):878–897. [PubMed: 31626364]
3. Stokum JA, Kwon MS, Woo SK, et al. SUR1-TRPM4 and AQP4 form a heteromultimeric complex that amplifies ion/water osmotic coupling and drives astrocyte swelling. Glia. 2018;66(1):108–125. [PubMed: 28906027]

4. Wang YF, Parpura V. Central role of maladapted astrocytic plasticity in ischemic brain edema formation. Front Cell Neurosci. 2016;10:129. [PubMed: 27242440]
5. Wang YF, Hatton GI. Astrocytic plasticity and patterned oxytocin neuronal activity: dynamic interactions. J Neurosci. 2009;29(6):1743–1754. [PubMed: 19211881]
6. Li D, Li T, Yu J, et al. Astrocytic modulation of supraoptic oxytocin neuronal activity in rat dams with pup-deprivation at different stages of lactation. Neurochem Res. 2020.
7. Illarionova NB, Gunnarson E, Li Y, et al. Functional and molecular interactions between aquaporins and Na, K-ATPase. Neuroscience. 2009.168(4):915–925. [PubMed: 19962432]
8. Theodosis DT, Poulain DA, Oliet SH. Activity-dependent structural and functional plasticity of astrocyte-neuron interactions. Physiol Rev. 2008;88(3):983–1008. [PubMed: 18626065]
9. Wang SC, Parpura V, Wang YF. Astroglial regulation of magnocellular neuroendocrine cell activities in the supraoptic nucleus. Neurochem Res. 2020. .
10. Choe KY, Prager-Khoutorsky M, Farmer WT, Murai KK, Bourque CW. Effects of salt loading on the morphology of astrocytes in the ventral glia limitans of the rat supraoptic nucleus. J Neuroendocrinol. 2016;28(4). https://pubmed.ncbi.nlm.nih.gov/26813227/doi:10.1111/jne.12370.
11. Wang Y-F, Liu L-X, Yang H-P. Neurophysiological involvement in hypervolemic hyponatremia-evoked by hypersecretion of vasopressin. Transl Biomed. 2011;2(2):3.
12. Yagil C, Sladek CD. Osmotic regulation of vasopressin and oxytocin release is rate sensitive in hypothalamoneurohypophysial explants. Am J Physiol. 1990;258(2 Pt 2):R492–R500. [PubMed: 2309938]
13. Wang YF, Sun MY, Hou Q, Parpura V. Hyposmolality differentially and spatiotemporally modulates levels of glutamine synthetase and serine racemase in rat supraoptic nucleus. Glia. 2013;61(4):529–538. [PubMed: 23361961]
14. Tweedle CD, Hatton GI. Synapse formation and disappearance in adult rat supraoptic nucleus during different hydration states. Brain Res. 1984;309(2):373–376. [PubMed: 6541076]
15. Salm AK, Smithson KG, Hatton GI. Lactation-associated redistribution of the glial fibrillary acidic protein within the supraoptic nucleus. An immunocytochemical study. Cell Tissue Res. 1985;242(1):9–15. [PubMed: 2412700]
16. Gottipati MK, Bekyarova E, Brenner M, Haddon RC, Parpura V. Changes in the morphology and proliferation of astrocytes induced by two modalities of chemically functionalized single-walled carbon nanotubes are differentially mediated by glial fibrillary acidic protein. Nano Lett. 2014;14(7):3720–3727. [PubMed: 24875845]
17. Wang YF, Hatton GI. Dominant role of betagamma subunits of G-proteins in oxytocin-evoked burst firing. J Neurosci. 2007;27(8):1902–1912. [PubMed: 17314286]
18. Mola MG, Sparaneo A, Gargano CD, et al. The speed of swelling kinetics modulates cell volume regulation and calcium signaling in astrocytes: a different point of view on the role of aquaporins. Glia. 2015;64(1):139–154. https://pubmed.ncbi.nlm.nih.gov/26413835/. [PubMed: 26413835]
19. Armstrong WE, Wang L, Li C, Teruyama R. Performance, properties and plasticity of identified oxytocin and vasopressin neurones in vitro. J Neuroendocrinol. 2010;22(5):330–342. [PubMed: 20210845]
20. Brown CH, Bourque CW. Mechanisms of rhythmogenesis: insights from hypothalamic vasopressin neurons. Trends Neurosci. 2006;29(2):108–115. [PubMed: 16330104]
21. Hatton GI, Li Z. Mechanisms of neuroendocrine cell excitability. Adv Exp Med Biol. 1998;449:79–95. [PubMed: 10026788]
22. Armstrong WE, Stern JE. Electrophysiological distinctions between oxytocin and vasopressin neurons in the supraoptic nucleus. Adv Exp Med Biol. 1998;449:67–77. [PubMed: 10026787]
23. Hatton GI. Emerging concepts of structure-function dynamics in adult brain: the hypothalamoneurohypophysial system. Prog Neurogibol. 1990;34(6):437–504.
24. Prager-Khoutorsky M, Bourque CW. Osmosensation in vasopressin neurons: changing actin density to optimize function. Trends Neurosci. 2010;33(2):76–83. [PubMed: 19963290]
25. Petkovic F, Campbell IL, Gonzalez B, Castellano B. Reduced cuprizone-induced cerebellar demyelination in mice with astrocyte-targeted production of IL-6 is associated with chronically activated, but less responsive microglia. J Neuroimmunol. 2017;310:97–102. [PubMed: 28778453]

26. Pasantes-Morales H, Alavez S, Sanchez Olea R, Moran J. Contribution of organic and inorganic osmolytes to volume regulation in rat brain cells in culture. Neurochem Res. 1993;18(4):445–452. [PubMed: 8097294]
27. Zhang Z, Bourque CW. Osmometry in osmosensory neurons. Nat Neurosci. 2003;6(10):1021–1022. [PubMed: 12973356]
28. Pasantes-Morales H, Tuz K. Volume changes in neurons: hyperexcitability and neuronal death. Contrib Nephrol. 2006;152:221–240. [PubMed: 17065815]
29. Wang P, Qin D, Wang YF. Oxytocin rapidly changes astrocytic GFAP plasticity by differentially modulating the expressions of pERK 1/2 and protein kinase A. Front Mol Neurosci. 2017;10:262. [PubMed: 28860967]
30. Hussy N, Deleuze C, Desarmenien MG, Moos FC. Osmotic regulation of neuronal activity: a new role for taurine and glial cells in a hypothalamic neuroendocrine structure. Prog Neurogibol. 2000;62(2):113–134.
31. Wang YF, Sun MY, Hou Q, Hamilton KA. GABAergic inhibition through synergistic astrocytic neuronal interaction transiently decreases vasopressin neuronal activity during hypoosmotic challenge. Eur J Neurosci. 2013;37(8):1260–1269. [PubMed: 23406012]
32. Verbalis JG. Brain volume regulation in response to changes in osmolality. Neuroscience. 2010;168(4):862–870. [PubMed: 20417691]
33. Zhang B, Glasgow E, Murase T, Verbalis JG, Gainer H. Chronic hypoosmolality induces a selective decrease in magnocellular neurone soma and nuclear size in the rat hypothalamic supraoptic nucleus. J Neuroendocrinol. 2001;13(1):29–36. [PubMed: 11123513]
34. Pekny M, Wilhelmsson U, Bogestal YR, Pekna M. The role of astrocytes and complement system in neural plasticity. Int Rev Neurobiol. 2007;82:95–111. [PubMed: 17678957]
35. Ikeshima-Kataoka H, Abe Y, Yasui M. Aquaporin 4-dependent expression of glial fibrillary acidic protein and tenascin-C in activated astrocytes in stab wound mouse brain and in primary culture. J Neurosci Res. 2015;93(1):121–129. [PubMed: 25174305]
36. Benfenati V, Caprini M, Dovizio M, et al. An aquaporin-4/transient receptor potential vanilloid 4 (AQP4/TRPV4) complex is essential for cell-volume control in astrocytes. Proc Natl Acad Sci USA. 2011;108(6):2563–2568. [PubMed: 21262839]
37. Jiao R, Cui D, Wang SC, Li D, Wang YF. Interactions of the mechanosensitive channels with extracellular matrix, integrins, and cytoskeletal network in osmosensation. Front Mol Neurosci. 2017;10:96. [PubMed: 28424587]
38. Craven PA, DeRubertis FR. Effects of extracellular sodium on cytosolic calcium, PGE2 and cAMP in papillary collecting tubule cells. Kidney Int. 1991;39(4):591–597. [PubMed: 1646907]
39. Hatton GI. Function-related plasticity in hypothalamus. Annu Rev Neurosci. 1997;20:375–397. [PubMed: 9056719]
40. Yu YQ, Chen XF, Yang Y, Yang F, Chen J. Electrophysiological identification of tonic and phasic neurons in sensory dorsal root ganglion and their distinct implications in inflammatory pain. Physiol Res. 2014;63(6):793–799. [PubMed: 25157654]
41. Ghamari-Langroudi M, Bourque CW. Muscarinic receptor modulation of slow afterhyperpolarization and phasic firing in rat supraoptic nucleus neurons. J Neurosci. 2004;24(35):7718–7726. [PubMed: 15342739]
42. Kirchner MK, Foehring RC, Callaway J, Armstrong WE. Specificity in the interaction of high-voltage-activated Ca(2+) channel types with Ca(2+)-dependent afterhyperpolarizations in magnocellular supraoptic neurons. J Neurophysiol. 2018;120(4):1728–1739. [PubMed: 30020842]
43. Haam J, Popescu IR, Morton LA, et al. GABA is excitatory in adult vasopressinergic neuroendocrine cells. J Neurosci. 2012;32(2):572–582. [PubMed: 22238092]
44. Bacova Z, Kiss A, Jamal B, Payer J Jr, Strbak V. The effect of swelling on TRH and oxytocin secretion from hypothalamic structures. Cell Mol Neurobiol. 2006;26(4–6):1047–1055. [PubMed: 16625432]
45. Kuwahara S, Maeda S, Ardiles Y, et al. Immunohistochemical localization of aquaporin-4 in the rat pituitary gland. J Vet Med Sci. 2010;72(10):1307–1312. [PubMed: 20484841]
46. Mesbah-Benmessaoud O, Benabdesselam R, Hardin-Pouzet H, Dorbani-Mamine L, Grange-Messent V. Cellular and subcellular aquaporin-4 distribution in the mouse neurohypophysis and

the effects of osmotic stimulation. J Histochem Cytochem. 2011;59(1):88–97. [PubMed: 21339176]

47. Hatton GI, Perlmutter LS, Salm AK, Tweedle CD. Dynamic neuronal-glial interactions in hypothalamus and pituitary: implications for control of hormone synthesis and release. Peptides. 1984;5(Suppl 1):121–138. [PubMed: 6384946]
48. Stokum JA, Mehta RI, Ivanova S, Yu E, Gerzanich V, Simard JM. Heterogeneity of aquaporin-4 localization and expression after focal cerebral ischemia underlies differences in white versus grey matter swelling. Acta Neuropathol Commun. 2015;3:61. [PubMed: 26419740]
49. Paterson JA, Leblond CP. Increased proliferation of neuroglia and endothelial cells in the supraoptic nucleus and hypophysial neural lobe of young rats drinking hypertonic sodium chloride solution. J Comp Neurol. 1977;175(4):373–390. [PubMed: 915032]
50. Armstrong WE, Foehring RC, Kirchner MK, Sladek CD. Electrophysiological properties of identified oxytocin and vasopressin neurones. J Neuroendocrinol. 2019;31(3):e12666.

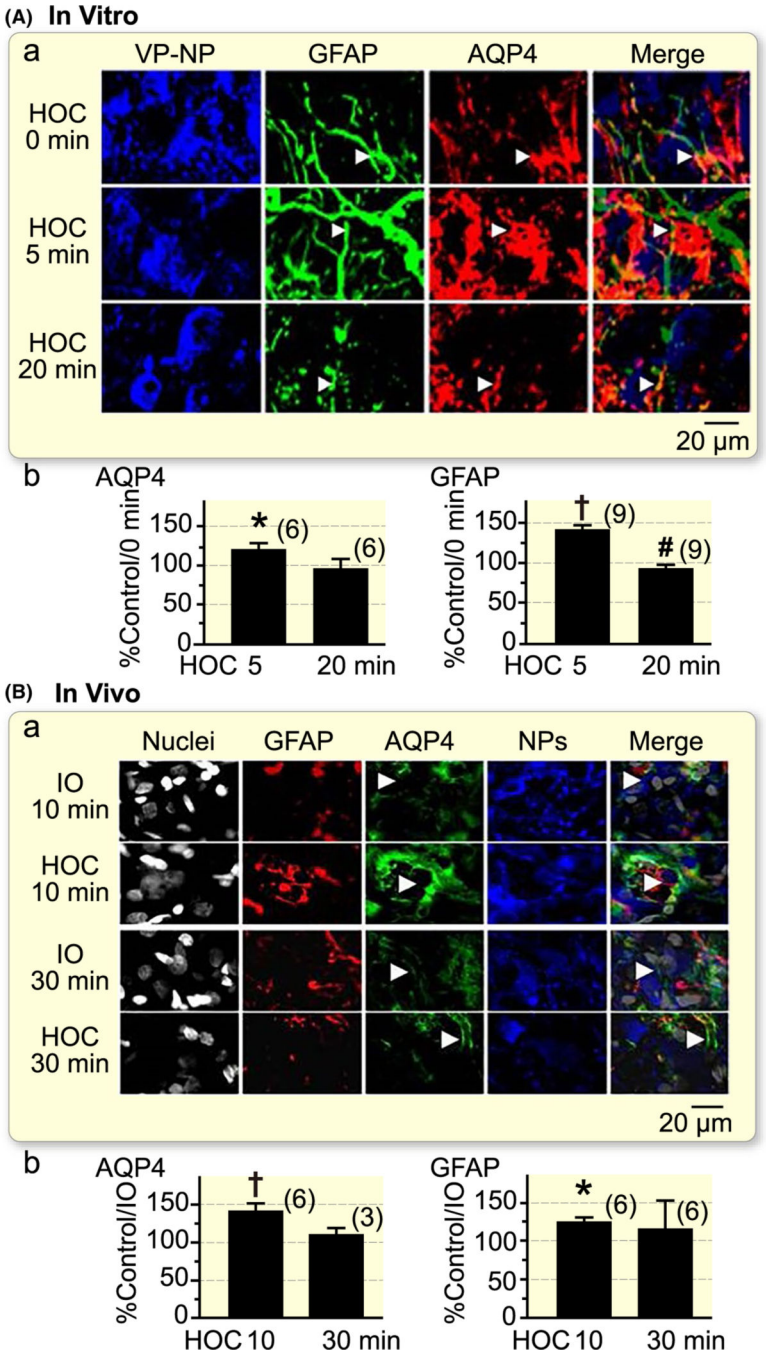

FIGURE 1.

Hyposmotic challenge (HOC) in rat supraoptic nucleus (SON) causes an increased staining of aquaporin 4 (AQP4) in regions containing glial fibrillary acidic protein (GFAP). A, Representative confocal images of the SON in vitro (acute brain slices, a) showing immunostaining of vasopressin-neurophysin (VP-NP), GFAP, AQP4 and their merges at immediately (0 min) before, and 5 min and 20 min under HOC (275 mOsm/kg, artificial cerebrospinal fluid), respectively. White arrowheads mark astrocytic somata (top row), processes (middle row) and end feet surrounding a blood vessel (bottom row). Ab. The bar

graphs summarize the percent changes in the expression of AQP4 stain (left panel) and GFAP filaments (right panel) at 5 min and 20 min relative to 0 min under HOC. B, Representative images showing effects after 10 min (a, top two panels) and 30 min (a, bottom two panels) of HOC in vivo (i.p.) relative to their corresponding controls (305 mOsm/kg saline or iso-osmolality, IO). White arrowheads at 10 min indicate astrocyte processes around SON magnocellular neuronal somata; the arrowheads at 30 min point to end feet surrounding a blood vessel. Bb. The bar graphs summarize the percent changes in the expression of AQP4 stain (left panel) and GFAP filaments (right panel) at 10 min and 30 min under HOC, respectively. $^{*}P < .05$; $^{\dagger}P < .01$ when compared to controls; $^{\#}P < .05$ compared to 5 min

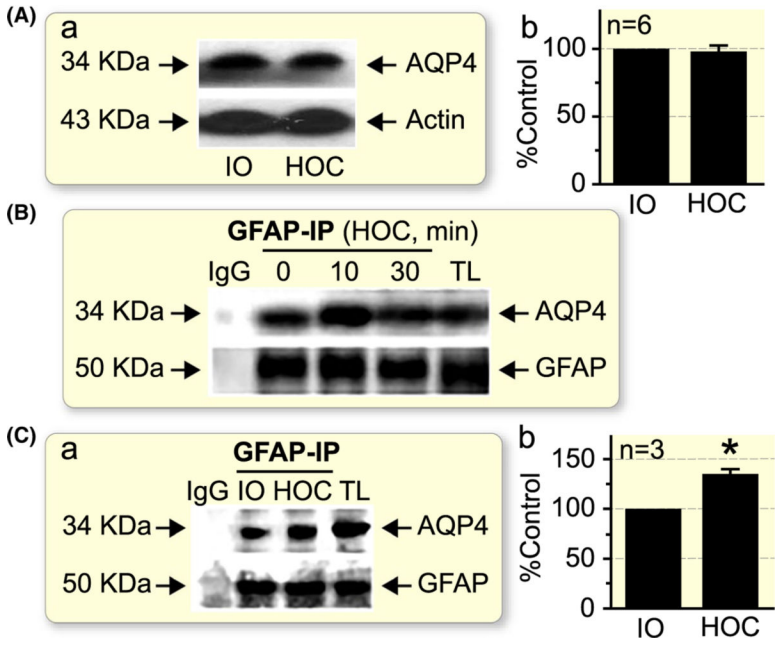

FIGURE 2.

HOC does not change the total amount of AQP4 in the SON, albeit it transiently increases molecular association of AQP4 with GFAP. A, A lack of effect by 10 min HOC in vivo on total AQP4 levels in the SON when compared to iso-osmotic (IO) control. B, Co-immunoprecipitation (IP) of GFAP with AQP4 in the SON after HOC in vivo at different time points. C, Comparison of co-immunoprecipitation of GFAP with AQP4 in the SON 10 min after in vivo HOC with control IO treatment. *$P < .05$ when compared to IO control. In A and C, panels show representative Western blots (a) and summary graph (b), expressed as a percentage of the AQP4 level in matching controls; n, sample size. Arrows indicate estimated molecular weight of the proteins. Actin was used as a loading control. IgG and total lysate (TL): negative and positive controls respectively

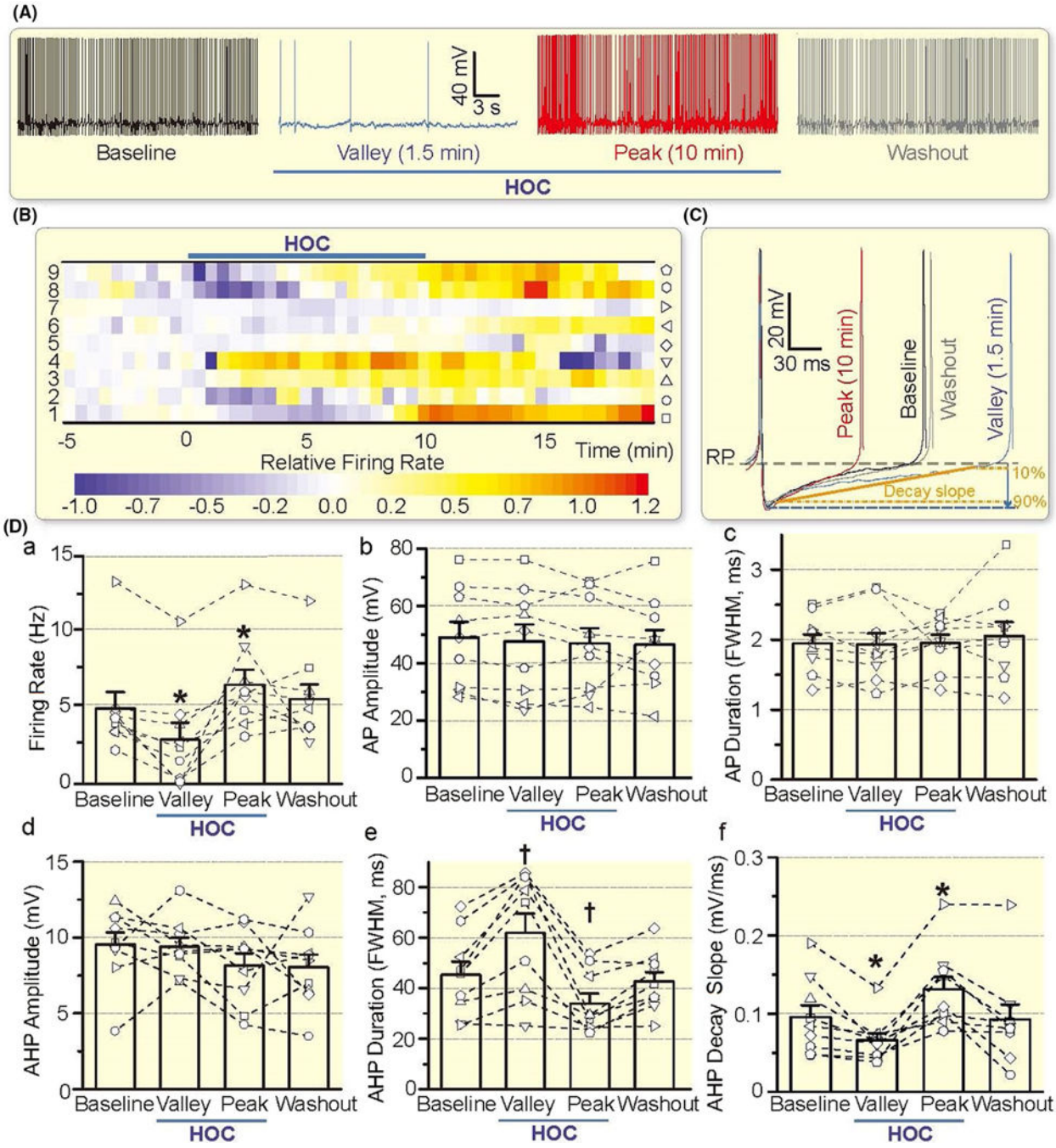

FIGURE 3.

HOC has dual effect on VP neuronal activity. A, Representative firing activity of a VP neuron (whole-cell patch-clamp recording) at control/baseline, 1.5 min and 10 min of HOC, and 10 min of washout, which correspond to the firing rate 1 min before HOC, the lowest firing rate (Valley), a rebound increase (Peak) of the firing rate during HOC and return to the baseline upon washout respectively. B, Heatmap of the relative firing rate showing the effect of HOC on the firing activity of VP neurons. Look-up table at the bottom indicates linear scale of relative firing rates, expressed as $(f - f_0)/f_0$, where f_0 was the baseline firing rate.

Symbols associated with individual VP neurons (numbered on the left) are shown in the vertical to the right. C, Representative action potentials/spikes at different stages of HOC; the resting membrane potential (RP) is indicated by the purple horizontal dashed line. Decay slope of AHP is defined based on 90% and 10% values (between solid and dashed lines in orange) of the AHP peak amplitude, the latter indicted by blue arrow and horizontal dashed line. D, Bar graphs illustrating the effect of HOC on the firing rate (a), action potential (AP) amplitude (b) and duration (c; expressed as FWHM), and afterhyperpolarization (AHP) amplitude (d), duration (e) and decay slope (f). $^{*}P < .05$ and $^{\dagger}P < .01$ compared with baseline value before HOC treatment by Bonferroni test

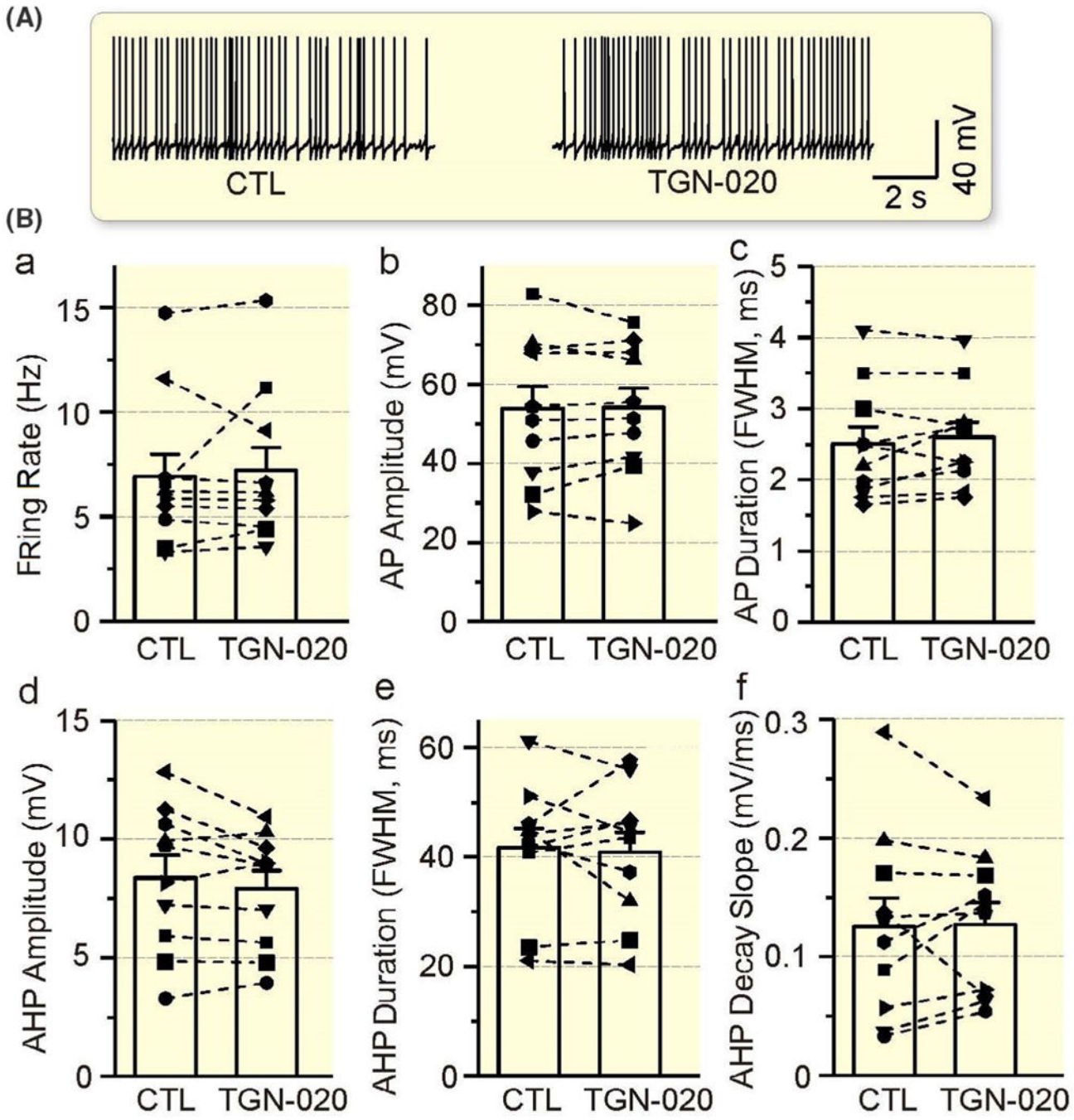

FIGURE 4.

Lack of significant effects of 2-(nicotinamide)-1,3,4-thiadiazole (TGN-020) on the electrical activity of VP neurons. A, Representative episodes of the firing activity of VP neurons in the presence of TGN-020 (10 μmol/L, 10 min) in patch-clamp recording, taken at 1 min before and 10 min after TGN-020 respectively. B, Bar graphs illustrating the lack of significant effect of TGN-020 on the firing rate (a), AP amplitude (b) and duration (c), and AHP amplitude (d), duration (e) and decay slope (f) in comparison to the control (CTL)

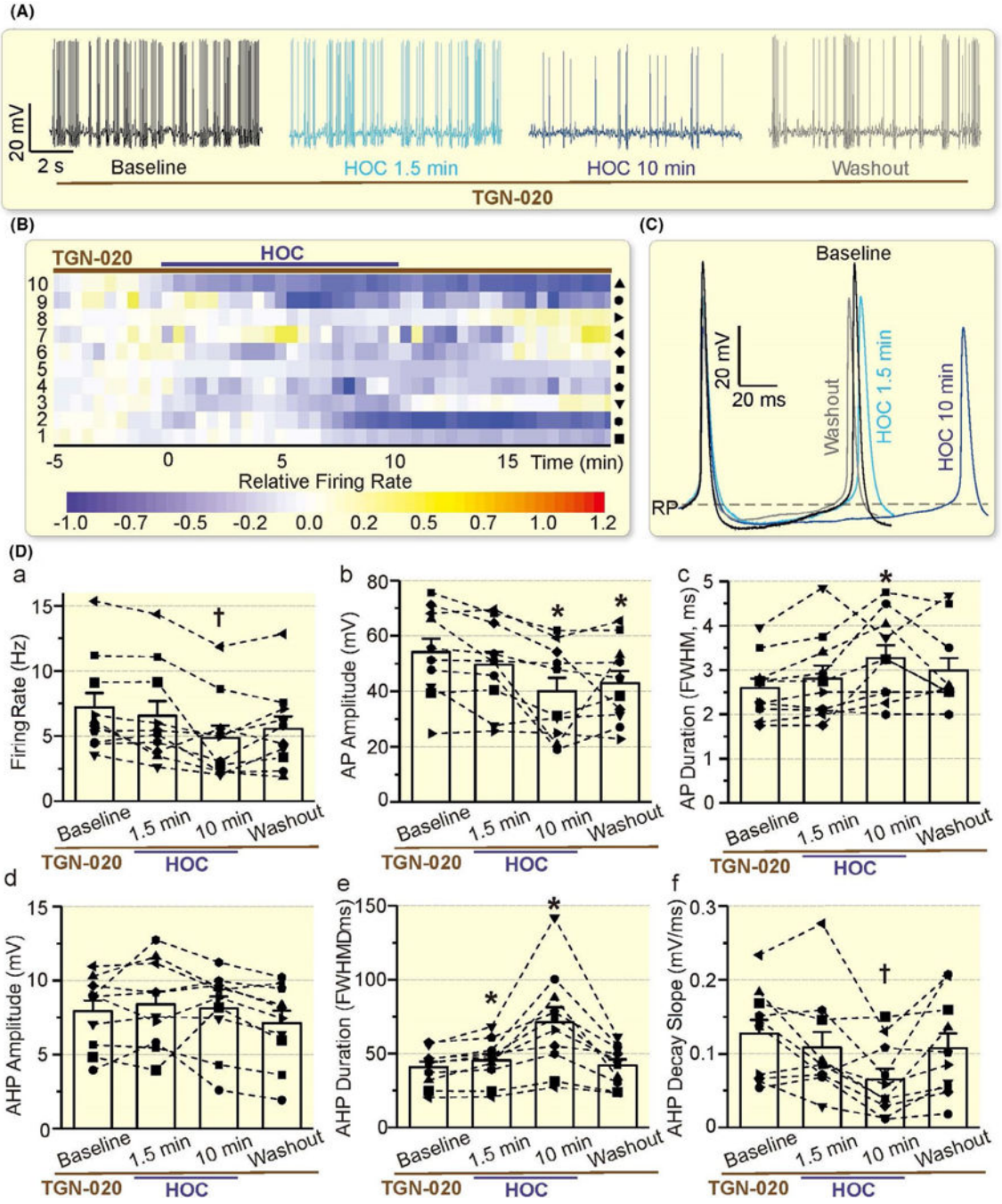

FIGURE 5.

Effects of TGN-020 on HOC-elicited inhibition and rebound excitation of VP neurons. A, Representative episodes of the firing activity of VP neurons in the presence of TGN-020 (10 μmol/L, 10 min before HOC) in patch-clamp recording, taken at 1 min before HOC, 1.5 min and 10 min after HOC and washout for 10 min, respectively. B, Heatmap of the relative firing rate shows the effect of HOC on 10 recorded VP neurons in the presence of TGN-020. C, Representative action potentials at different stages of HOC in the presence of TGN-020. D, Bar graph summarizing the effect of TGN-020 on HOC-evoked changes in the firing rate

(a), AP amplitude (b) and duration (c; expressed as FWHM), and AHP amplitude (d), duration (e) and decay slope (f).

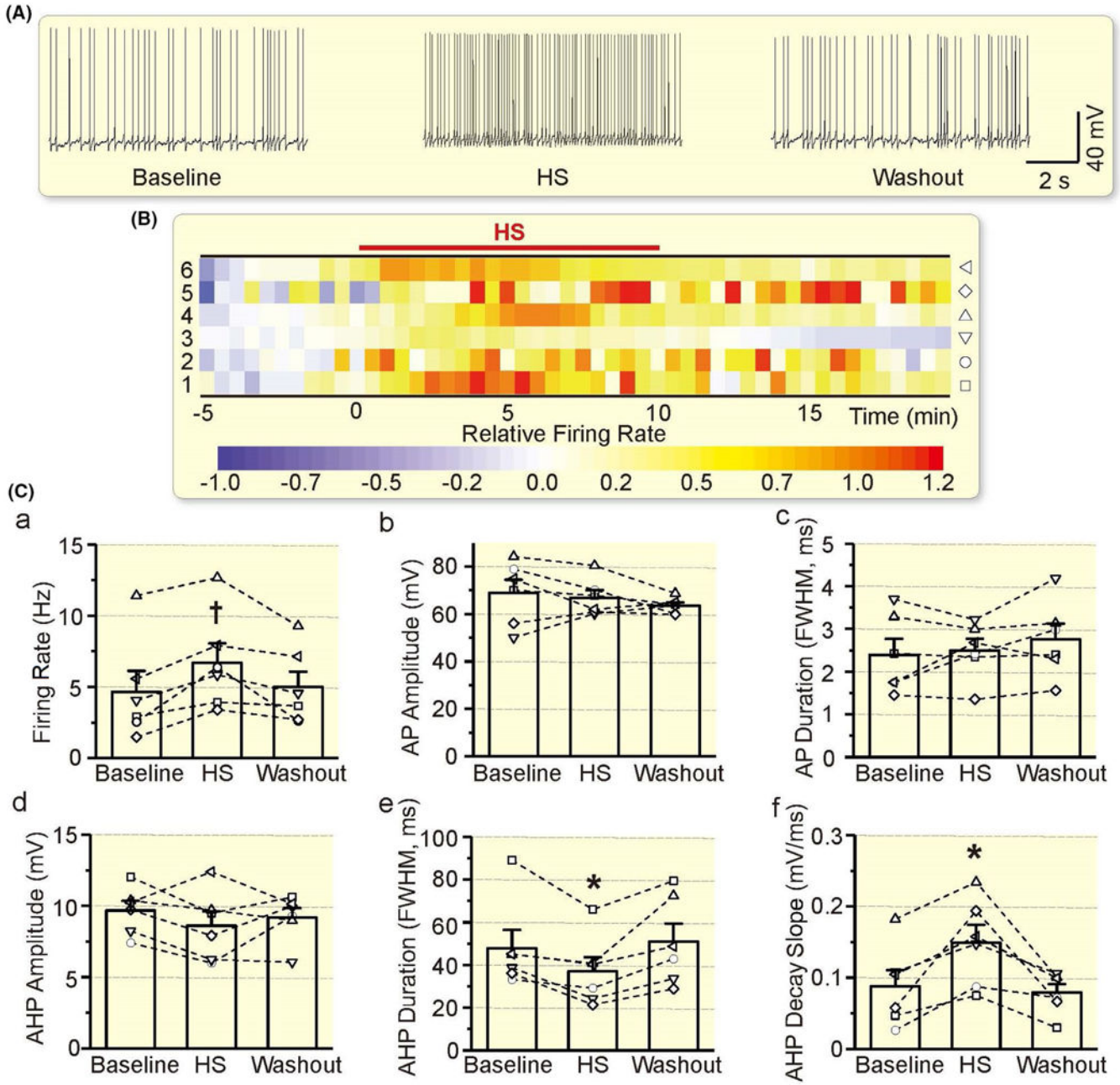

FIGURE 6.

Effects of hyperosmotic stress (HS) on the electrical activity of VP neurons. A-C, Representative episodes (A), heatmap of the relative firing rate (B) and summarizing bar graphs (C) of the electrical activity of VP neurons in patch-clamp recording, taken at 1 min before HS, 10 min after HS and washout for 10 min respectively. Other annotations refer to Figures 3 and 5

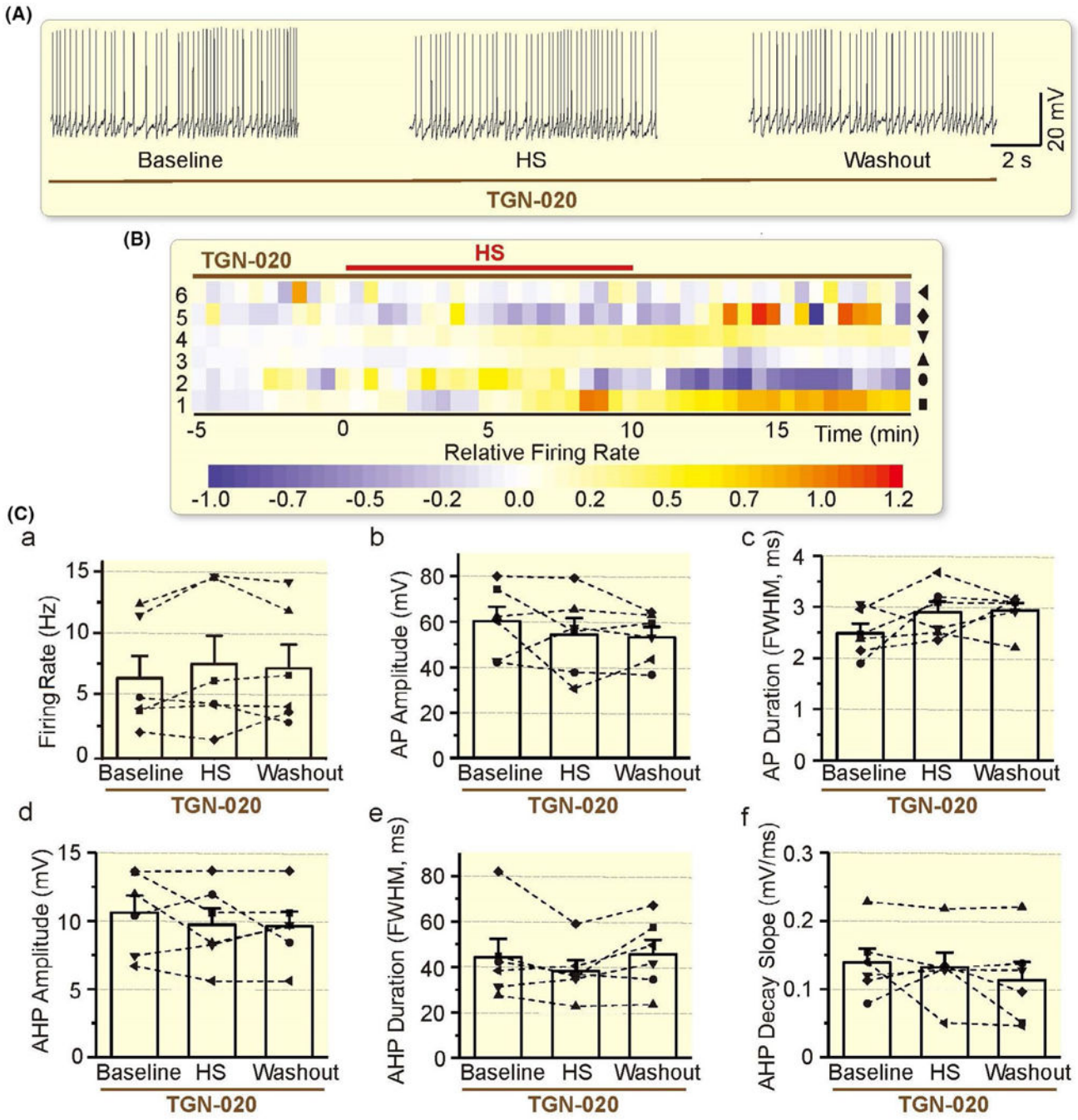

FIGURE 7.

Effects of AQP4 blockage on HS-elicited excitation of VP neurons. A-C, Representative episodes (A), heatmap of the relative firing rate (B) and summarizing bar graphs (C) of the electrical activity of VP neurons in the presence of TGN-020 (10 μmol/L, 10 min before HS) in patch-clamp recording, taken at 1 min before HS, 10 min after HS and washout for 10 min respectively. Other annotations refer to Figures 3, 5 and 6

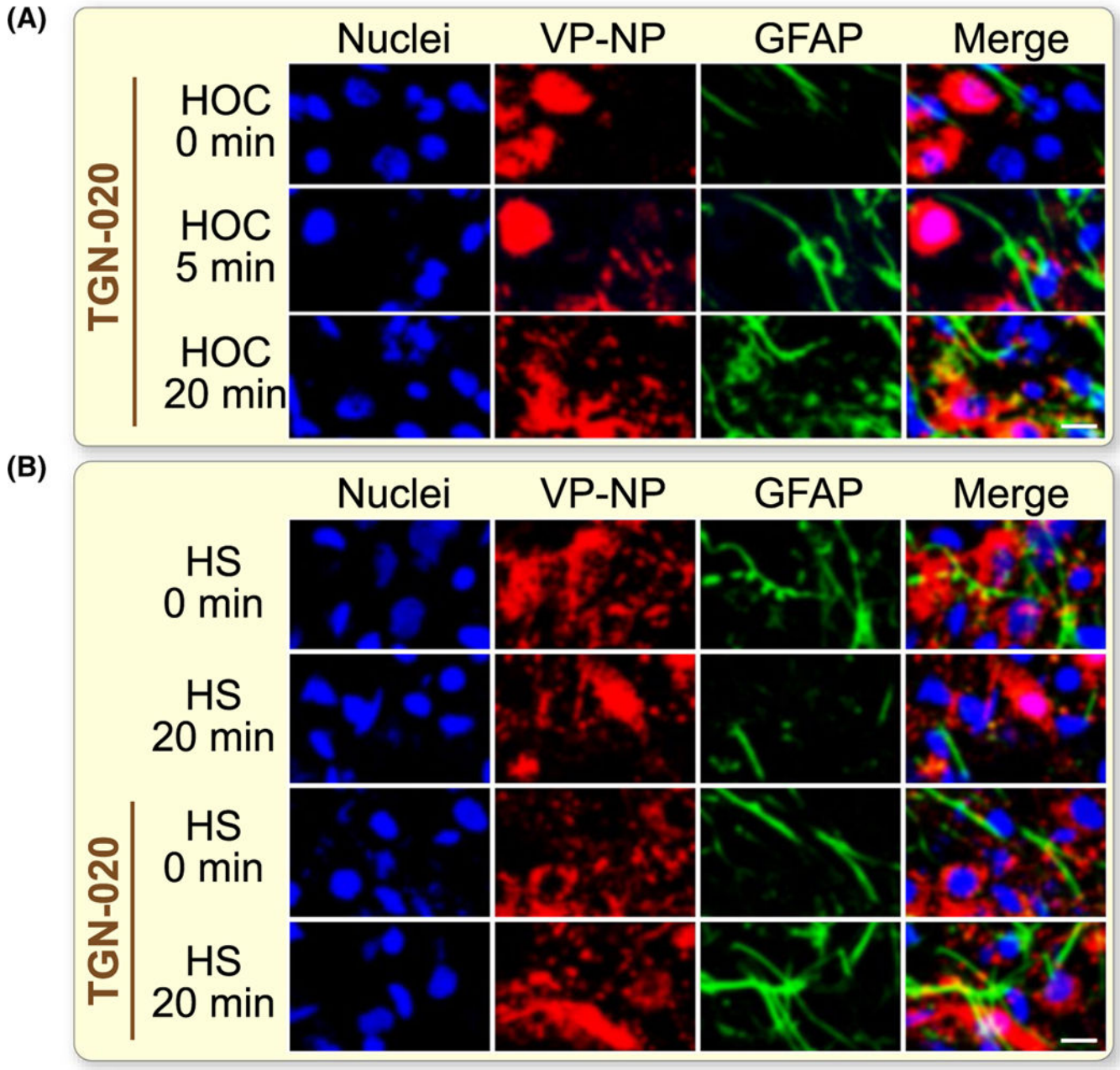

FIGURE 8.

Effects of blocking AQP4 activity on osmotic stimuli-evoked GFAP filament retraction in the SON. A, Representative fluorescence images of SON slices treated with HOC for 0, 5 and 20 min in the presence of TGN-020 respectively. B, Confocal microscopic images following HS in the absence (top two rows) and the presence of TGN-020 (bottom two rows) for 0 min and 20 min, respectively. The white scale bars equal 20 μm. For other annotations refer to Figure 1

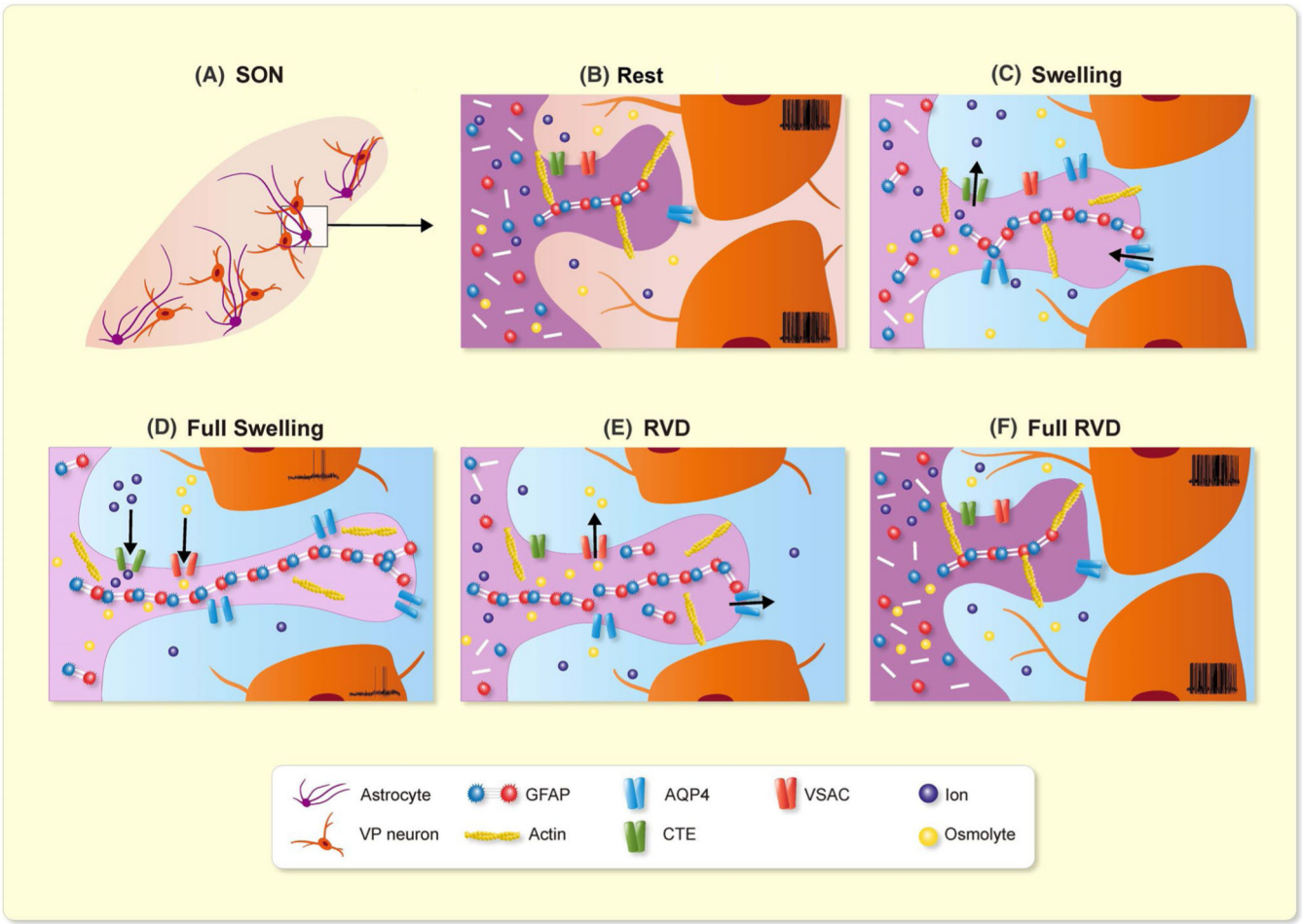

FIGURE 9.

Hypothetic mechanisms underlying dual astrocytic plasticity and VP neuronal response to HOC. A, Model of the histological relationship between astrocytes and VP neurons in the SON; B, Before HOC (Rest); C, Initial HOC (Swelling); D, Full swelling; E, Transition to regulatory volume decrease (RVD); F, Full RVD. CTE, ion channels, transporters and exchangers; VSAC, volume-sensitive anion channels